# Sequential Processes to Produce N-$TiO_2$ Films Through Rf Plasmas

R Valencia-Alvarado[1,a], A de la Piedad-Beneitez[2,b], R López-Callejas[1,c], B G Rodríguez-Méndez[1,d],A Mercado-Cabrera[1,e], R Peña-Eguiluz[1,f], A E Muñoz-Castro[1,g] and J M de la Rosa-Vázquez[3,h]
[1]Instituto Nacional de Investigaciones Nucleares, Plasma Physics Laboratory, AP 18-1027, 11801, México, D.F., México
[2]Instituto Tecnológico de Toluca, AP 890, Toluca, México
[3]ESIME-Zacatenco-IPN, AP 07738, México, D.F., México
[a]raul.valencia@inin.gob.mx[1], [b]anibal.delapiedad@gmail.com, [c]regulo.lopez@inin.gob.mx, [d]benjamin.rodriguez@inin.gob.mx, [e]antonio.cabrera@inin.gob.mx, [f]rosendo.eguiluz@inin.gob.mx, [g]arturo.munoz@inin.gob.mx, [h]mdelaros@ipn.mx

**Abstract.** Using as target a CpTi disk in an atmosphere of argon/oxygen and by rf plasma. First titanium dioxide ($TiO_2$) films were obtained on silicon substrates, and subsequently, these films were doped with nitrogen (N-$TiO_2$). In both processes, along four hours at 390°C of temperature. X-Ray diffraction and Raman spectroscopy confirmed the presence of the nanostructured anatase phase. X-ray photoelectron spectroscopy analyzes indicate that the nitrogen atoms were incorporated into the $TiO_2$ film with ~33.9 at%. The films reach a thickness of 1.25 μm and 40 nm the average uniformity determined by using an atomic force microscope. Finally, UV-Vis diffuse reflectance spectroscopy outcome evaluated ones an energy band gap reduction from 3.17 eV to 2.95 eV corresponding to $TiO_2$ films and N-$TiO_2$ films respectively.

## 1. Introduction

Titanium dioxide ($TiO_2$) is nowadays one of the materials most researched as an efficient photocatalyst for the photodegradation of pollutants in waste water owing to its high oxidizing power, non-toxicity and long-term photostability [1]. However, the practical application of $TiO_2$ is severely limited by its band gap of 3.2 eV in crystalline anatase phase, which facilitates response to only ultraviolet light accounting for less than 5% of the solar spectrum. To expand the widespread use of $TiO_2$, is necessary to absorb visible light [2], [3], [4]. Thus, any change in the optical response of $TiO_2$ has a positive effect on its photocatalytic efficiency of this.

Up to date, with the aim to improve $TiO_2$ photocatalytic activity, various investigations have been conducted, and this is achieved by doping the $TiO_2$ with non-metallic elements such as nitrogen. The nitrogen-doped $TiO_2$ (N-$TiO_2$) can be obtained by various methods

* Corresponding author: authorraul.valencia@inin.gob.mx

such as sol-gel [5], visible-light-active [6], low temperature hydrothermal [7], cathodic magnetron [8], etc.

In this work aimed to obtain N-$TiO_2$ films on silicon substrates, it proceeded in two steps. Firstly the growth of $TiO_2$ films through an rf plasma in an argon-oxygen atmosphere and sputtering from a DC biased CpTi disk; secondly, the N-$TiO_2$ films by using an rf plasma discharge in a nitrogen environment.

## 2. Experimental Setup

The $TiO_2$ and N-$TiO_2$ processes were carried out in a cylindrical Pyrex-type glass chamber (diameter 20 cm and long 50 cm) coupled to a vacuum system. A base pressure $1\times10^{-4}$ mbar was reached and subsequently with the working gas admission raised up to $5\times10^{-2}$mbar. The plasma discharge was generated by an RF source (13.56 MHz) matched to a solenoidal antenna coiled on the glass chamber.

The process was realized on a silicon substrate in two steps. Firstly, the plasma was created in an argon-oxygen mixture aiming to obtain a $TiO_2$ and a commercially pure titanium (CpTi) cylindrical target of 9 mm in diameter and 5 mm long, previously situated in the chamber. The CpTi is negatively biased by a DC power supply during four hours to increase ions collisions on the target, promoting material sputtering and its consequent oxidation process. From this process, some of the titanium dioxides produced are deposed over an electrically floated silicon substrate, placed on a holder at 2 cm in front of the target. The ion bombardment raised the target temperature around 290°C without bias and increased up to ~700°C when the target was biased at -3 kV and the temperature on the substrate was established, in the range from 290°C (without biased target) to 390°C (with biased target). In the second stage, a 100% nitrogen gas was used, with the same conditions of temperature in the target to those obtained in the first step.

The composition and structure of the films have been characterized using different techniques. The atomic percentage of nitrogen-oxygen-titanium films was evaluated by X-ray photoelectron spectroscopy (XPS) using a Thermo K-alpha XPS system with AlKα radiation. Crystalline phases of the films on the substrates surface were detected by X-ray diffraction (XRD) using a Siemens D5000 X-ray diffractometer under the following operational conditions: 40 kV acceleration voltage and 39 mA, angular range $20° \leq 2\theta \leq 90°$ and step time 2s; the phases were identified with the help of JCPDS files. The near surface phases by micro-Raman spectroscopy model Lab-Ram-HR Horiba Yobin-Yvon using a Nd:Y Ag laser with 532 nm wavelength. The thickness of the film was accomplished with the KLA-TenKor AlphaStep D-120 Stylus Profiler. The topographical information about the films by atomic force microscope (AFM) was providing. Finally, the band gap was determined by UV-Vis/diffuse reflectance spectroscopy (DRS) technique using Perkin Elmer spectrophotometer, operating at 200 to 1100 nm window, width 1nm steps and scan speed of 480 nm/min.

## 3. Results and Discussion

XPS studies of chemical oxidation states titanium (Fig. 1.a) and N-$TiO_2$ (Fig. 1.b) are determined. The elements detected after this process are C, N, O and Ti; and the atomic composition of each one corresponds to 4.10, 33.90, 9.63 and 52.37 at% respectively. The carbon in the film of N-$TiO_2$ is attributed to doping species and produced by the evolution of the wall of the chamber where they carry out the experiments. The change in the spectra of N-$TiO_2$ (Fig. 1.b) with respect to $TiO_2$ (Fig. 1.a) is evident, well confirmed the effectiveness of nitrogen doping on the silicon substrate.

The high-resolution XPS spectrum of Ti-2p is showed in Fig. 1.c. In this figure exhibits the deconvolution and peak fitting realized by Ti-2p core level of N-$TiO_2$ film. The binding energies for Ti-$2p_{3/2}$ located in 458 eV and Ti-$2p_{l/2}$ located in 464 eV. The compounds for the Ti-$2P_{3/2}$ are integrated by: a) Ti atoms bonded to oxygen like in $TiO_2$ located in 457.5 eV [9], 458.5 eV [10] and 459.1 eV [11] binding energies; b) Ti atoms bonded to nitrogen like in TiN found in 454.8 eV [10], 455.6 eV [12] and 456.3 eV [13] binding energies. The compounds for the Ti-$2P_{1/2}$ are composed for: a) the Ti-N bonds in 460.6 eV [14], 461 eV [15] and 462.2 eV [16] binding energies; b) $TiO_2$ bonds with 463.6 eV [17], 464.0 eV [17] and 465.5 eV [18] binding energies.

The XPS high-resolution spectrum of the N1s region were performed on the surface shown in Fig. 1.d with the aim of investigating the chemical state of the nitrogen atom in N-$TiO_2$. Expanding the range of binding energies of 393-401 eV, two peaks corresponding to the doping species introduction during the nitriding process, this agrees with the comments by other authors [19], [20]. A significant peak is around 396.6 eV, and lower intensity in the 397.5 eV both the TiN [21] are attributed. Two peaks located at 395.2 eV and 396 eV assigned to the NC bonds in the TiN [22], [6], [7]. Finally, the peak located at 399.2 eV is attributed to link N-C-O in $TiO_2$ [23]. These doping can induce the formation of new energy level in the band gap of $TiO_2$.

The XPS spectrum in the region O1s showed in Fig. 1.e, this is deconvoluted into seven peaks. a) 529.6 eV and 530.5 eV these peaks corresponding to $TiO_2$ and are in accordance with other authors [24], [17], [25]. b) The corresponding peak at 528.4 eV possibly the mixture of $O_2$-oxo [24]. c) 531.5 eV and 534.4 eV these peaks are attributable to OH group [17]; this, suggested a possible contamination introduced in the cleaning process due to us using the isopropyl alcohol, similar results have been obtained by Regnini *et al* [26]. Finally d) 532.3 eV and 533.3 eV corresponding to surface active oxygen in O-C groups [25].

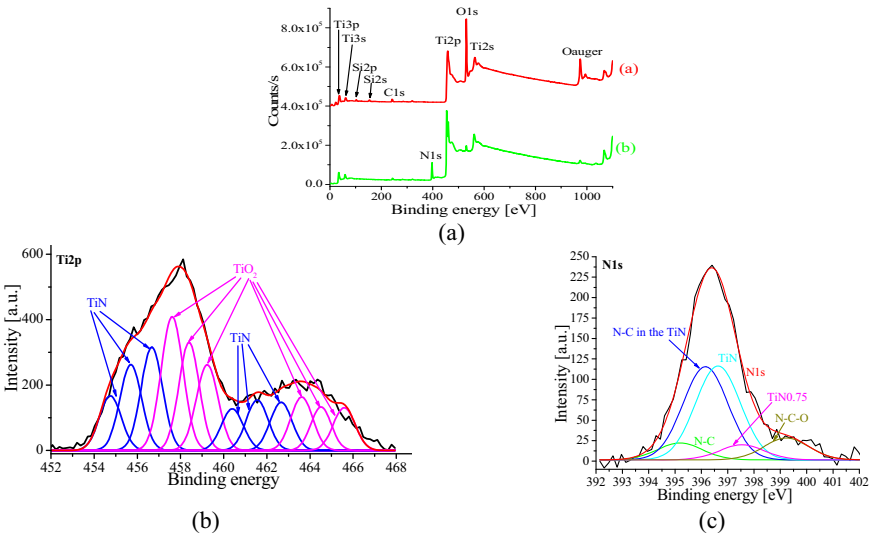


(a)

(b)

(c)

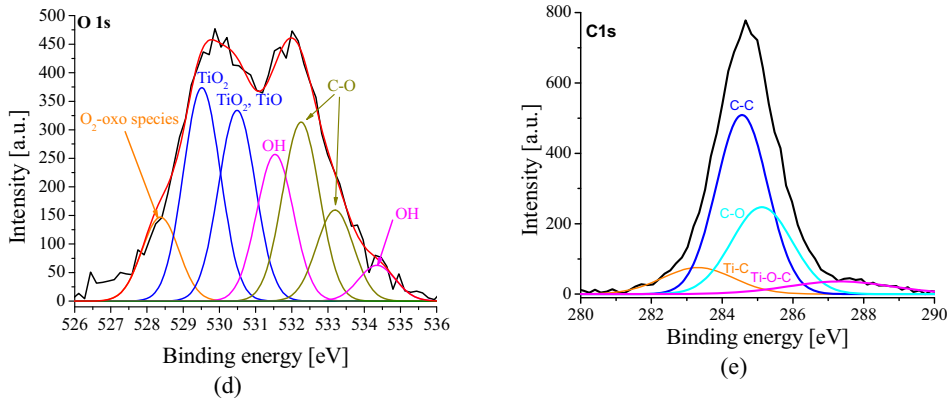


**Fig. 1**. XPS spectra of a) $TiO_2$ control, b) N-$TiO_2$ in Si substrate, c) Ti2p, d) N1s, e) O1s, and, e) C1s.

The XPS spectrum in the C1s region is showing in Fig. 1.f, this is deconvoluted into four peaks. The dominant C1s at 284.4 eV could be attributed to C-C bond [27]. The coexistence of peaks centred at 283.2 eV, 285.0 eV and 287.6 eV may correspond to the energies of Ti-C, C═O and Ti-O-C bond [28]. This result indicates the presence interstitial C as well as C atoms substitution of Ti and O atoms in the $TiO_2$ lattice.

Figure 2 shows depth profile of atomic percentage obtained by the XPS etching depth of the film of $TiO_2$ nitrogen-doped. In this figure, the initial concentration of the carbon is high ~54at.% and quickly decreases as well oxygen, which has an initial percentage of ~23at.%. While that XPS etching depth up to 1800 s profiles titanium increased the atomic percentage of the depth and nitrogen more or less remains constant.

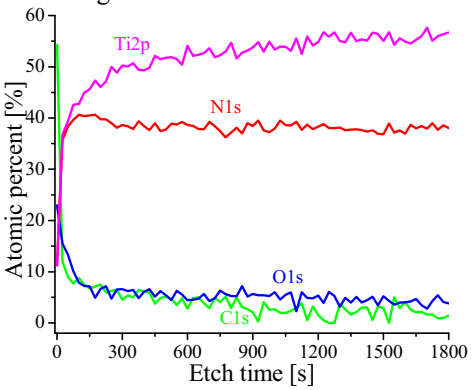


**Fig. 2**. Shows the XPS depth profile carried out by XPS by sputtering etching to the nitrogen-doped $TiO_2$ film.

Figure 3 shows the spectrum obtained by X-ray diffraction from N-$TiO_2$ deposited on the silicon substrate. The spectrum clearly shows that the predominant crystalline phases are those of the anatase $TiO_2$, with the diffraction peaks at 2θ=25.3°, 37.0°, 37.8°, 38.6°, 48.1°, 55.2°, 62.8°, 75.2° and 82.9°, corresponding to the reflections from 101, 103, 004, 112, 200, 211, 204, 215 and 224 crystal planes in accordance to JCPDS No. 21-1272 files, similar results has been obtained by Ong *et al* [25]. In the spectrum is shown a small peak due to the rutile phase in 27.5° corresponding to reflection 110 [20]. With the maximum intensity of anatase and rutile peaks was determined the percent values, so, corresponding to 93.88% anatase and 6.12% rutile. It suggested, that the substitution of N ions in the lattice of $TiO_2$ did not induce the formation of nitrogen impurities in the anatase phase, similar results has been obtained by others authors [29], [30] and [25]. The crystallite sizes

of anatase were determined using Sherrer equation, in the most intensive peaks, resulting 21.3 nm and 35.5 nm for $TiO_2$ and N-$TiO_2$ respectively.

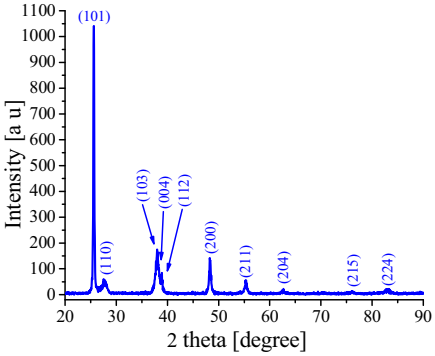


**Fig. 3.** X-ray diffraction N-$TiO_2$ silicon substrate.

Figure 4 shows the Raman spectrum on silicon substrate, which confirms the presence of the anatase phase in both layers of $TiO_2$ and N-$TiO_2$. These results are indicative of the low temperature at which is performed the two process and are consistent with XRD studies. Also, the silicon substrate does not exhibit links of nitrogen with oxygen or titanium. In the spectra of Fig.4, can be observed the vibration bands corresponding to $E_{1g}$, $B_{1g}$, $A_{1g}$, and $E_{2g}$, Raman modes and intensities of each peak are showed in Table 1. It is remarkable that the $E_{1g}$ vibration band, it is very intense and acute, similar conditions have been reported by other researchers [31], [28], [25]. In Table 1 shows that after the doping process with nitrogen, the N-$TiO_2$ film has a vibrational band right shifted, indicating that the particle size has been increased, this effect has been observed by others authors [32], [33]. Later is consistent with the results of XRD.

**TABLE 1.** RAMAN SHIFT VALUES AND PEAK INTENSITIES

| | $E_{1g}$/Intensity | $B_{1g}$/Intensity | $A_{1g}$/Intensity | $E_{2g}$/Intensity | Ratio $A_{1g}/E_{1g}$ |
|---|---|---|---|---|---|
| $TiO_2$ | 144/2953.83 | 399/247.48 | 519/336.56 | 639/443.72 | 11.39 % |
| N-$TiO_2$ | 150/3420.34 | 401/389.91 | 525/391.66 | 642/496.09 | 11.45 % |

The $E_{1g}$ peak is associated with the symmetric stretching vibration of O-Ti-O in $TiO_2$, the $B_{1g}$ peak is due to the symmetric bending vibration of O-Ti-O [34], and the $A_{1g}$ peak is the result of antisymmetric bending vibration of O-Ti-O [35]. Considering the proposed by Fang Tian *et al* [34], the ratio of the Raman vibrational modes intensities between $E_{1g}$ and $A_{1g}$ for $TiO_2$ and N-$TiO_2$ films, the percentage are approximately of 11%, i.e., the symmetric and antisymmetric vibrations remain without perceptible change.

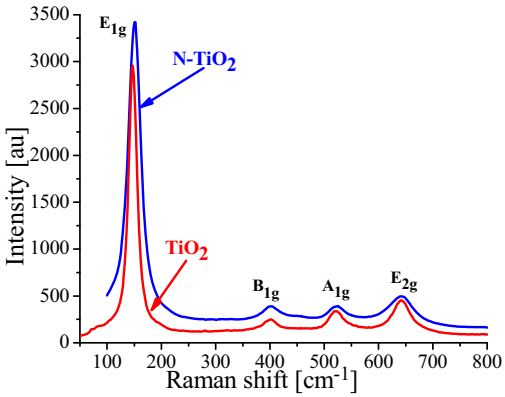


**Fig. 4**. Raman spectra of $TiO_2$ and N-$TiO_2$ films on silicon substrate.

Figure 5 shows the thickness measurement of the film doped with nitrogen carried out with the profilometer y correspond to ~1370 nm, similar results has been obtained by Hoang *et al.* [36].

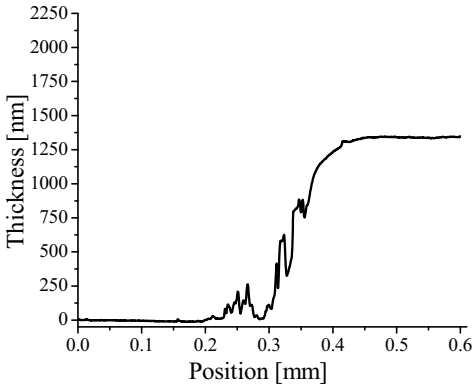


**Fig. 5.** Film thickness N-$TiO_2$

Finally, AFM was used to show the morphology and roughness surface of $TiO_2$ (Fig. 6.a) and
N-$TiO_2$ (Fig. 6.b) films. It is notorious that N-$TiO_2$ samples in both: grain size and roughness as been increased, compared with $TiO_2$ ones, Han *et al.* [37] and Kimiagar and Mohammadizadeh [38] have reported similar results. UV-Vis/DRS studies confirmed the improved light absorption of the N-$TiO_2$ by reducing the energy band gap from 3.17 to 2.95 eV (see Fig. 7), i.e., that the doping with nitrogen of the $TiO_2$ films causes the generation of oxygen vacancies, thus making a contribution to visible light response.

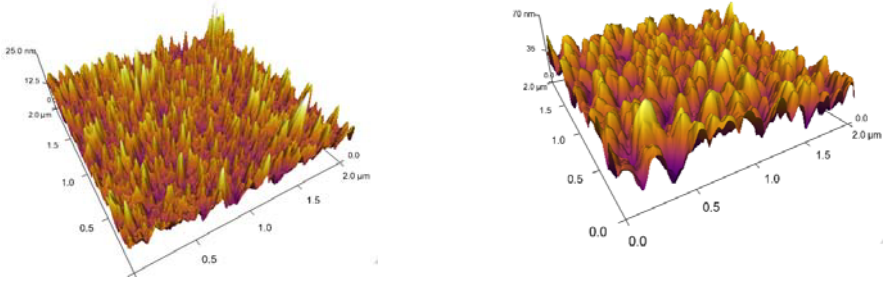

a) b)

**Fig. 6.** AFM images a) $TiO_2$ sample b) N-$TiO_2$ sample.

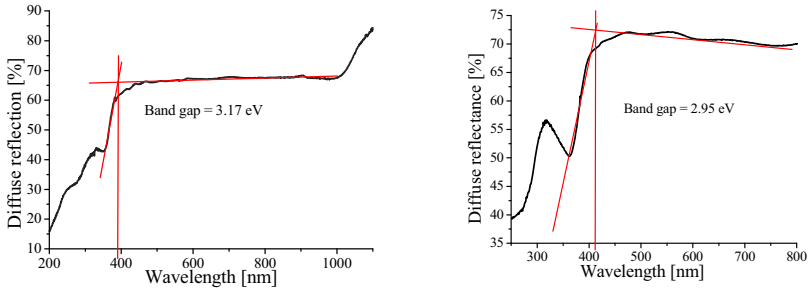


a) b)

**Fig. 7.** By UV-visible diffuse reflectance values of $E_g$ for: a) $TiO_2$, b) N-doped $TiO_2$.

## 4. Conclusions

Using a RF plasmas system and by sputtering of CpTi target, first in an atmosphere of argon-oxygen plasma were obtained $TiO_2$ films on silicon substrate. Later, in nitrogen plasma atmosphere was obtained N-$TiO_2$. Both processes were carried out at constant temperature of 390°C. The characterization of N-$TiO_2$ films on substrate by XPS confirms the formation of Ti-N and also, carbon species were identified such as Ti-C, C-O, C-C and Ti-O-C links, these indicating the penetration interstitial of C atoms in the anatase lattice. The anatase and rutile phases were determined by XRD studies with an obvious domain of anatase phase in the above in a ratio of 15: 1 for peak intensity. The crystallite sizes of anatase phase had an increase of ~60% with respect to $TiO_2$. According to the Raman spectra of $TiO_2$ and N-$TiO_2$, the anatase phase was corroborated. The vibrational bands of $E_{1g}$, $B_{1G}$, $A_{1g}$ and $E_{2g}$, they presented a Raman shift, this is attributed to the crystallite sizes growth. By means of AFM, a 40 nm average roughness on the surface of the samples treated with N-$TiO_2$ was determined. Also, a growth in grain size was observed. Finally, using UV-Vis/DRS it was determined that films after doped with nitrogen $TiO_2$ the band gap is reduced, thus achieving the films can respond to visible light.

## 5. Acknowledgments

This project has been partially founded by CONACyT-México. The authors are grateful to Dr. Manuel Espinoza for their technical support in the XRD diagnostic, Dr. Enrique Camps for Raman spectroscopy, Phys. Rafael Basurto for XPS spectroscopic and Chem. Pavel López for AFM studies. The technical assistance received from Pedro Ángeles Espinoza, María Teresa Torres M. and Isaías Contreras Villa is much appreciated.

## References

1. A. Sobczyk-Guzenda, H Szymanowski, W. Jakubowski, A. Błasińska, J. Kowalski, M. Gazicki-Lipman “Morphology, photocleaning and water wetting properties of cotton fabrics, modified with titanium dioxide coatings synthesized with plasma enhanced chemical vapor deposition technique”, Surf. & Coat. Tech. 217 (2013) 51-57.
2. J. Luo, S. K. Karuturi, L. Liu, L. T. Su, A. I. Y. Tok, H. J. Fan, “Homogeneous photosensitization of complex $TiO_2$ nanostructures for efficient solar energy conversion”, Sci. Rep. 2 (2012) 451.
3. G. Liu, L.Ch Yin, J. Wang, P. Niu, Ch. Zhen, Y. Xie, H.M. Cheng “A red anatase $TiO_2$ photocatalyst for solar energy conversion”, Energy Environ. Sci. 5 (2012) 9603.
4. J. Yu, J. Low, W. Xiao, P. Zhou, M. Jaroniec, “Enhanced photocatalytic $CO_2$ reduction activity of anatase $TiO_2$ by coexposed {001} and {101} facets” J. Am. Chem. Soc. 136-25 (2014) 8839-8842.

5. R. Rahimi, S. S. Moghaddam, M. Rabbani, "Comparison of photocatalysis degradation of 4-nitrophenol using N,S co-doped TiO2 nanoparticles synthesized by two different routes" J Sol-Gel Sci Technol 64 (2012) 17–26.
6. X Cheng, X Yu, Z Xing, J Wan, "Enhanced photocatalytic activity of nitrogen doped $TiO_2$ anatase nano-particle under simulated sunlight irradiation", Energy Procedia 6 (2012) 598-605.
7. N R Khalid, E Ahmed, Z Hong, Y Zhang, M Ahmad, "Nitrogen doped $TiO_2$ nanoparticles decorated on graphene sheets for photocatalysis applications", Curr. Appl. Phys. 12 (2012) 1485-1492.
8. K. Yamada, H. Yamane, S. Matsushima, H. Nakamura, T. Sonoda, S. Miura, K. Kumada "Photocatalytic activity of TiO2 thin films doped with nitrogen using a cathodic magnetron plasma treatment" Thin Solid Films 516 (2008) 7560-7564.
9. J Jin, S-Z Huang, J Liu, Y Li, L-H Chen, Y Yu, H-E Wang, C P Grey, and B-L Su, "Phases hybriding and hierarchical structuring of mesoporous $TiO_2$ nanowire bundles for high-rate and high-capacity lithium batteries", Adv. Sci. (2015) DOI: 10.1002/advs.201500070.
10. H Do, T-Ch Yen, and L Chang, "Stability and etching of titanium oxynitride films in hydrogen microwave plasma", Vac. Sci. Technol. A 31-4 (2013) 41304-1-7.
11. J. Senthilnathan and L Philip, "Investigation on degradation of methyl parathion using visible light in the presence of Cr+3 and N-doped TiO2", Adv. Mat. Res. Vols. 93-94 (2010) 280-283.
12. J Zhang, B Gao, Q Gan, J Xia, Y Cao, Y Ma, J Wang, K Huo, "Fabrication and capacitive properties of C-doped $TiO_2$ nanotube array" Chem. Rapid Commun. Vol 2-2 (2014) 29-32.
13. G Zheng, J Wang, X Liu, A Yang, H Song, Y Guo, H Wei, Ch Jiao, S Yang, Q Zhu, Z Wang, "Valence band offset of MgO/$TiO_2$ (rutile) heterojunction measured by X-ray photoelectron spectroscopy", Appl. Surf. Sci. 256 (2010) 7327-7330.
14. T Hu, Ch Chu, Y Xin, S Wu, K W K Yeung, P K. Chu, "Corrosion products and mechanism on NiTi shape memory alloy in physiological environment" Mater. Res., 25-2 (2010) 350-358.
15. M Tallarida, Daniel Friedrich, Matthias Städter, Marcel Michling, and Dieter Schmeisser, "Growth of $TiO_2$ with thermal and plasma enhanced atomic layer deposition", J. of Nanoscience and Nanotechnology, 11 (2011) 1-5.
16. W Zhang, T Hu, B Yang, P Sun, H He, "The effect of boron content on properties of B-$TiO_2$ photocatalyst prepared by Sol-gel method", J. Adv. Oxid. Technol. 16-2 (2013) 261-267.
17. V-D Dao, L L Larina, and H-S Choi, "Plasma reduction of nanostructured $TiO_2$ electrode to improve photovoltaic efficiency of dye-sensitized solar cells", J. of the Electrochem. Soc., 161-14 (2014) H896-H902.
18. X. Xia, Z. Zeng, X. Li, Y. Zhang, J. Tu, Ch. Fan, H. Zhang, H. J. Fan, "Fabrication of metal oxide nanobranches on atomic-layer-deposited $TiO_2$ nanotube arrays and their application in energy storage" Nanoescale 5 (2013) 6040-6047.
19. G Liu, F Li, D-W, D-M Tang, Ch Liu, X Ma, G Q Lu and H-M Cheng, "Electron field emission of a nitrogen-doped TiO2 nanotube array", Nanotechnol. 19 (2008) 025606.
20. Z Xiaoyan, S Peng, C Xiaoli, "Nitrogen-doped $TiO_2$ photocatalysts synthesized from titanium nitride: characterizations and photocatalytic hydrogen evolution performance", J. of Adv. Oxid. Technol., 16-1 (2013) 131-136.
21. Ch Chen, H Bai, S-M Chang, Ch Chang and W Den, "Preparation of N-doped TiO2 photocatalyst by atmospheric pressure plasma process for VOCs decomposition under UV and visible light sources", J. of Nanoparticle Res. (2007) 9:365–375.

22. Y-Ch Lin, Ch-Y Lin, and P-W Chiu, "Controllable graphene N-doping with ammonia plasma", Appl. Phys. Lett. 96 (2010) 133110.
23. X-J Zou, K N Ding, Y F Zhang, and J Q Li, "A DFT study of acetonitrile adsorption and decomposition on the $TiO_2$ (110) surface", Int. J. of Quantum Chem., 111-5 (2011) 915-922.
24. L. Yang, Z. Jiang, S. Lai, Ch. Jiang, and H. Zhong, "Synthesis of titanium containing SBA-15 and its application for photocatalytic degradation of phenol", Int. Journal of Chem. Eng., 2014 (2014) 691562
25. W-J Ong, L-L Tan, S-P Chai, S-T Yong, and A R Mohamed, "Self-assembly of nitrogen-doped $TiO_2$ with exposed {001} facets on the graphene scaffold as photo-active hybrid nanostructures for reduction of carbon dioxide to methane", Nano-Res. 7-10 (2014) 1528–1547.
26. D. Regonini, A. Jaroenworaluck, R. Stevensa and C.R. Bowen, "Effect of heat treatment on the properties and structure of TiO2 nanotubes: phase composition and chemical composition", Surf. Interface Anal. 42, (2010) 139–144
27. J Sun, H Zhang, L-H Guo, and L Zhao, "Two-dimensional interface engineering of a titania-graphene nanosheet composite for improved photocatalytic activity", Appl. Mater. Interfaces 5 (2013) 13035-13041
28. G. Liu, Ch. Han, M. Pelaez, D. Zhu, S Liao, V. Likodimos, N. Ioannidis, A. G. Kontos, P. Falaras, P. S. M. Dunlop, J. A. Byrne and D. D. Dionysiou, "Synthesis, characterization and photocatalytic evaluation of visible light activated C-doped $TiO_2$ nanoparticles", Nanotechnology 23 (2012) 294003.
29. E. Finazzi, C. Di Valentin, A. Selloni, G. Pacchioni, "First principles study of nitrogen doping at the anatase $TiO_2$(101) surface", J. Phys. Chem. C, 111-26 (2007) 9275–9282.
30. F. Peng, L. Cai, H. Yu, H. Wang, J. Yang, "Synthesis and characterization of substitutional and interstitial nitrogen-doped titanium dioxides with visible light photocatalytic activity" J. of Solid State Chem. 181 (2008) 130–136
31. Q Xiang, J Yu, M. Jaroniec, "Synergetic effect of $MoS_2$ and graphene as cocatalysts for enhanced photocatalytic $H_2$ production activity of $TiO_2$ nanoparticles", J. Am. Chem. Soc. 134 (2012) 6575-6578.
32. G. Yang, Z. Jiang, H. Shi, T. Xiao, Z. Yan, Preparation of highly visible-light active N-doped $TiO_2$ photocatalyst, J. Mater. Chem., 20 (2010) 5301–530.
33. N. M. Thuy, D. Q. Van, L. T. Hong-Hai, The visible light activity of the $TiO_2$ and TiO2:V4+ photocatalyst, Nanomater nanotechnol., 2 (2012) 14:2012.
34. F Tian, Y Zhang, J Zhang, and Ch Pan, "Raman spectroscopy: a new approach to measure the percentage of anatase $TiO_2$ exposed (001) facets", J. Phys. Chem. C 116 (2012) 7515−7519
35. JR Huang, X Tan, T Yu, L Zhao, WL Hu, Enhanced photoelectrocatalytic and photoelectrochemical properties by high-reactive $TiO_2/SrTiO_3$ hetero-structured nanotubes with dominant {001} facet of anatase $TiO_2$, Electroch. Acta 146 (2014) 278-287.
36. S Hoang, S Guo, N T. Hahn, A J. Bard, and C. B Mullins, "Visible light driven photoelectrochemical water oxidation on nitrogen-modified $TiO_2$ nanowires", Nano Lett. 12 (2012) 26-32.
37. L Han, Y Xin, H Liu, X Ma, G Tang, "Photoelectrocatalytic properties of nitrogen doped TiO2/Ti photoelectrode prepared by plasma based ion implantation under visible light", J. of Hazard. Mat. 175 (2010) 524–531.
38. S Kimiagar, and M R Mohammadizadeh, "N-doped TiO2 nanothin films: photocatalytic and hydrophilicity properties", Eur. Phys. J. Appl. Phys. 61 (2013) 10303.